

**SYNTHESIS, CHARACTERIZATION AND ANTIMICROBIAL
SCREENING OF ZnS/CdS/NiS NANOCOMPOSITE PREPARED
BY PRECIPITATION METHOD**

MSc GRAGUATE PROJECT

KENNO BENTI GASISA

**OCTOBER 2016
HARAMAYA UNIVERSITY, HARAMAYA**

**Synthesis, Characterization and Antimicrobial Screening of ZnS/CdS/NiS
Nanocomposite Prepared by Precipitation Method**

**MSc Graduate Project Submitted to the Department of Chemistry,
Postgraduate Program Directorate
HARAMAYA UNIVERSITY**

**In Partial Fulfillment of the Requirement for the Degree of
MASTER OF SCIENCE IN CHEMISTRY (INORGANIC CHEMISTRY)**

Kenno Benti Gasisa

**October 2016
Haramaya University, Haramaya**

DEDICATION

This graduate project manuscript is dedicated to my beloved families for nursing me with affection and love and for their dedicated partnership in the success of my life.

STATEMENT OF THE AUTHOR

By my signature below, I declare and affirm that this Graduate Project is my own work and I have followed all ethical and technical principles of scholarship in the preparation, data collection, data analysis and complication of this project. Any scholarly matter that in Graduate Project has been given recognition through citation.

This Graduate project is submitted in partial fulfillment of the requirements for an MSc Degree at the Haramaya University. The Graduate Project is deposited in the Haramaya University Library and is made available to borrowers under the rules of the Library. I solemnly declare that this Graduate Project has not been submitted to any other institution any whereby for the award of any academic degree, diploma or certificate.

Brief quotations from this Graduate project may be allowed without special permission provided that accurate and complete acknowledgment of source is made. Requests for extended quotations from or reproduction of this Graduate project in whole or in part may be granted by head of Department when in his or her judgment the proposed use of material is in the interests of scholarship. In all other instances, however, permission must be obtained from the author of the Graduate project.

Name: **Kenno Benti Gasisa**

Signature: _____

Date: _____

Department: **Chemistry**

BIOGRAPHICAL SKETCH OF THE AUTHOR

The author was born on June 10, 1983 in Kobera Birbir Kebele, Guliso Woreda, West Wollega Gimbi zone of the Oromia Regional State. He attended his primary education at Gulliso Elementary School from 1990-1998 and Secondary Education at Lalo Ayira Secondary School (LASS) from 1999-2002.

In 2003 he joined Adama Teachers college and received his diploma in Chemistry in July 2005. He was employed as Teacher at Lalo Ayira Secondary School (LASS), in September 2006. He then taught for two years at Guliso Secondary and Preparatory School and joined Jimma University in 2007 and graduated with B.Ed in chemistry in November 2010 and then joined Haramaya University, Post Graduate Program Directorate, College of Computational and Natural Science, Department of Chemistry in 2012 to pursue his MSc in Chemistry (Inorganic Chemistry).

ACKNOWLEDGEMENTS

First of all, I am greatly indebted to my Almighty God for helping me to complete this research work and for all His help throughout my life.

I am deeply indebted to my advisor Dr. Tesfahun Kebede for his invaluable and stimulating interest and unreserved support most generously given during the course of my study. I pay respect and express indebtedness to him because of his guidance, consistent supervision as well as suggestions in every phase of this project work.

I am very thankful to my wife Derartu Tsega, Kebena Wayina, Gadisa Amenu, Mengistu Itefa Adamu Wayina, Ayana Tolesa and Megarsa Abdi for their technical support and fruitful assistance, which invariably helped me a lot during this research work.

I am also gratefully to the Chemistry Department of Haramaya University, Dr. Abi Taddese, Dr. Endale Teju and Mr. Zewdu Bezu for hosting me to pursue my MSc study. My sincere thanks is also due to Mr. Fituma Diriba, Chemistry Laboratory Assistance, who arranged a work place and provided me with all necessary apparatus during the course of this project work.

My special thanks is also due to Prof. Dr. Rer.Nat. habil. Gyeong-Man Kim, Head Department of Material Engineering at Adama Science and Technology University for his assistance in conducting the XRD measurements on my research samples.

ACRONYMS AND ABBREVIATIONS

Ev	Electron volt
DI	Deionized
Eg	Band Gap Energy
JCPDS	Joint Committee on Powder Diffraction Standards
MHA	Mueller Hinton Agar
NPs	Nano Particles
SEM	Scanning Electron Microscopy
TEM	Transmission Electron Microscopy
Uv-Vis	Ultra Violet Visible
XRD	X-ray Diffraction

TABLE OF CONTENTS

STATEMENT OF THE AUTHOR	iv
BIOGRAPHICAL SKETCH OF THE AUTHOR	v
ACKNOWLEDGEMENTS	vi
ACRONYMS AND ABBREVIATIONS	vii
TABLE OF CONTENTS	viii
LIST OF TABLES	x
LIST OF FIGURES	xi
LIST OF TABLE IN THE APPENDIX	xii
ABSTRACT	xiii
1. INTRODUCTION	1
2. REVIEW OF RELATED LITERATURE	5
2.1. Applications and Uses of Nanotechnology	5
2.2. Applications and Properties of Nanoparticles	6
2.3. Methods of Synthesis of Metal Sulfide and Mixed Metal Sulfide	7
2.4. Applications and properties of Metal Sulfides (II-VI) Semiconductors	9
2.4.1. Zinc Sulfide (ZnS)	9
2.4.2. Cadmium Sulfide (CdS)	9
2.4.3. Nickel Sulfide (NiS)	10
2.5. Antimicrobial activities of Metal sulfide Nanomaterials	11
2.5.1 Zinc Sulfide (ZnS)	11
2.5.2. Cadmium Sulfide (CdS)	12
2.5.3. Nickel Sulfide (NiS)	12
3. MATERIALS AND METHODS	14
3.1. Experimental Site	14
3.2. Materials and Apparatus	14
3.2.1. Chemicals and Reagents	14
3.2.2. Apparatus and Instruments	14
3.3. Synthesis Methods	15
3.3.1. Synthesis of ZnS Nanoparticles	15
3.3.2. Synthesis of CdS Nanoparticles	15

Continues...

3.3.3. Synthesis of NiS Nanoparticles	15
3.3.4. Synthesis of ZnS/CdS Nanocomposite	16
3.3.5. Synthesis of ZnS/NiS Nanocomposite	16
3.3.6. Synthesis of ZnS/CdS/NiS Nanocomposites.	16
3.4. Characterization Methods	17
3.4.1. Analysis of Uv-Vis Diffuse Reflectance Absorption Spectra	17
3.4.2. X-ray Diffraction Measurements	17
3.5. Antimicrobial Screening of the as- Synthesized Nanoparticles	18
3.5.1. Preparation of Media	18
3.5.2. Procedure for Anti-microbial Activity Test.	18
4. RESULTS AND DISCUSSION	19
4.1. Characterization of the as-Synthesized Nanomaterials	19
4.1.1. Analysis of Uv-Vis Diffuse Reflectance Absorption Spectra	19
4.1.2. Analysis of X-ray Diffraction Patterns of the Nanomaterials	22
4.2. Antimicrobial Activities of the As-synthesized Nanomaterials	24
5. SUMMARY, CONCLUSION AND RECOMMENDATIONS	29
5.1. Summary and Conclusion	29
5.2. Recommendation	30
6. REFERENCE	31
7. APPENDIX	36

LIST OF TABLES

Table	Page
1. Crystallite size (D) of as-synthesized nanomaterials	24
2. Zone of inhibition (in mm) nanomaterials	28

LIST OF FIGURES

Figure	Page
1. Tauc plots (a) ZnS, (b) CdS, (c) NiS, (d) ZnS/CdS, (e) ZnS/NiS and (f) ZnS/CdS/NiS nomaterials	20
2. The XRD patterns of the as-synthesized nanomaterials: (a) ZnS, (b) CdS, (c) NiS, (d) ZnS/CdS, (e) ZnS/NiS and (f) ZnS/CdS/NiS	22
3. Inhibition zone of as synthesized NPs against <i>Staphylococcus aureus</i> bacteria	25
4. Inhibition zone of as synthesized NPs against against <i>streptococcus</i> bacteria	26
5. Inhibition zone of as synthesized NPs against <i>Escherichia coli</i> bacteria	26
6. Inhibition zone of as synthesized NPs against <i>Pseudomonas aeruginosa</i> bacteria	27

LIST OF TABLE IN THE APPENDDIX

Appendix Table	Page
1. Wave length (nm) and absorbance (a.u) for Uv-Vis absorption spectrum of ZnS, CdS, NiS, ZnS/CdS, ZnS/NiS and ZnS/CdS/NiS	37

SYNTHESIS, CHARACTERIZATION AND ANTIMICROBIAL SCREENING OF ZnS/CdS/NiS NANOCOMPOSITE PREPARED BY PRECIPITATION METHOD

ABSTRACT

Nanoparticles of the metal sulfides (ZnS, CdS and NiS) were prepared by precipitation method from the aqueous solution of Na₂S. 9H₂O using aqueous solutions of their soluble salts Zn (NO₃)₂.6H₂O, Cd(NO₃)₂.4H₂O, Ni(NO₃)₂.4H₂O, respectively. Likewise the binary nanocomposites ZnS/CdS and ZnS/NiS were prepared by the same method, by mixing equimolar solutions of their precursors used for the preparation of ZnS and CdS as well as ZnS and NiS, respectively. Similarly, the ternary nanocomposite ZnS/CdS/NiS was prepared by mixing aqueous solution of their precursors used for the preparation of ZnS, CdS and NiS. All these as-synthesized nanomaterials were characterized using Uv-Vis Spectrophotometer and X-ray diffractometer. The band gap energy were obtained using Tauc plot. XRD patterns were recorded using a diffractometer equipped with a Cu target K radiation ($\lambda = 1.5401 \text{ \AA}$) source. Accordingly, the average crystallite size of ZnS/CdS/NiS nanocomposite was calculated based on the primary peak on its XRD patterns and found to be in the range of 2.5 and 9 nm. Finally antimicrobial activities of all the synthesized nanomaterials were studied against Gram positive (Staphylococcus aureus and Streptococcus) and Gram negative (Escherichia coli and Pseudomonas aeruginosa) bacteria using paper disc diffusion technique. Accordingly, ZnS/CdS/NiS nanocomposite exhibited a much better cumulative effect than the other as-synthesized nanoparticles and this value was almost comparable with that of, Chloramphenicol, a commercially available antibiotics. The binary nanocomposites ZnS/CdS and ZnS/NiS also showed significant antimicrobial activities better than their corresponding single components.

Key words: ZnS/CdS, ZnS/NiS, ZnS/CdS/NiS, Precipitation Methods and Antimicrobial Screening

1. INTRODUCTION

Nanocrystalline materials have attracted much attention in recent years because of properties in nano forms differ significantly from those of their bulk counterparts (Nanda and Sarma, 1999). Many fundamental properties of materials (optical, electrical, mechanical, *etc.*) can be expressed as a function of their size, composition and structural order (Senthilkumaar and Selvi, 2008). When the size of a semiconductor becomes comparable to the 1S-exciton diameter, they exhibit quantum confinement (Weller, 1993). This results in the appearance of a quantized Eigen spectrum and an increase in the energy gap relative to the band gap (E_g) of the bulk solid (Martinez *et al.*, 2010). Consequently, much effort has been made to control the size, morphology and crystallinity of nanocrystals with a view to tune their physical properties.

Nanocomposites derived from nano-scale inorganic/organic particles that are dispersed in a polymer matrix homogeneously have attracted considerable attention (Carotenuto *et al.*, 2014). The diverse and numerous polymers to choose from are well documented, including both plastics and elastomers, which are the main two types of polymers. Organic/inorganic hybrid materials offer highly interesting and versatile applications when incorporated with a polymer (Kaltenhauser *et al.*, 2013). Among the inorganic/polymer nano-composites, metal sulfides/polymer nanocomposites have been researched extensively due to their interesting optical, electrical and mechanical properties (Zhang *et al.*, 2012). Their excellent physical and chemical properties in various fields, such as catalysis, sensors, solar cells, photo detectors, light emitting diodes and laser communication, have made them very attractive and promising materials (Ranjbar *et al.*, 2013). Semiconductor particles immobilized in a polymer matrix with nano-scale grain size show different properties relative to the same material in bulk form because of quantum size effects (Singh *et al.*, 2010).

Group IIB–VI nanoparticles are important semiconductor compounds and one of the most explored because of their wide range of potential applications. ZnS has a wide direct band gap of 3.65 eV when bulk (Gao, 2004) and 3.82 eV in nanoscale (Olumide *et al.*, 2014), it is a promising material for optoelectronic device applications such as optical coatings, solid-state solar cell windows, electro optic modulators, photoconductors, field effect transistors, sensors, transducers, light-emitting applications, and photonic crystal devices which operate in the

region from visible to near infrared (Elidrissi *et al.*, 2001). On the other hand, CdS nanoparticle is the most studied system among all the II-VI semiconducting nanoparticles (Weller, 1993). It has relatively a wide band gap semiconducting material having band gap energy of 2.4 eV and this material is widely used because of its size dependent photophysical, photochemical and non-linear optical properties, etc. (Alivisatos, 1996).

Nickel sulfides (NiS) is another important member of transition metal family that can be used as potential applications in lithium ion batteries, as catalyst in the degradation of organic dyes, super capacitors and dye- sensitized solar cells. The different phases of nickel sulfide has more complex phases such as NiS (α -NiS and β -NiS), Ni₃S₂, NiS₂, Ni₃S₄, Ni₉S₈, and Ni₇S₆ which make synthesis of single-phase nickel sulfide complicated. NiS shows two different phase types, depending on the synthesis temperature. Ghezlbash *et al.*, (2004) reported that the phase transformation from α -NiS to β -NiS occurs at 282⁰C. It has band gap energy of 2.8 eV at high temperature calcination 1000⁰C (Alin *et al.*, 2015) and 0.15 eV in bulky (Atay, 2002).

There are various physical, chemical and biological methods for synthesizing semiconductor nanoparticles. CdS, ZnS and NiS nanoparticles have been synthesized by precipitation method from their respective metal precursors, i.e. cadmium nitrate, zinc acetate and nickel nitrate , and as a source of sulfur, sodium sulfide (Na₂S) was used (Shubhangi *et al.*, 2010). Some of the other techniques, which have been used for the preparation of nanoparticles includes solvothermal process, Uv irradiation, colloidal emulsion and sol-gel methods etc. A lot of works have been done on the synthesis of these nanoparticles, yet the chemical precipitation method is found to be the most suitable and accepted technique, because of the ability of the production of various sizes and large quantities of nanoparticles.

The emerging infectious diseases and the development of drug resistance in the pathogenic bacteria and fungi at an alarming rate is a matter of serious concern. Despite the increased knowledge of microbial pathogenesis and application of modern therapeutics, the morbidity and mortality associated with the microbial infections still remains high. Therefore, there is a pressing demand to discover novel strategies and identify new antimicrobial agents from natural and inorganic substances to develop the next generation of drugs or agents to control microbial infections. Prior to the extensive use of chemotherapeutics in modern health care system,

inorganic antimicrobials such as silver and copper were used since ancient times to treat microbial infections (Moghimi, 1999). In the recent years, due to the development of new strains, resistance of some bacteria to commonly used bactericide antibiotics has increased. Some of the antimicrobial agents, being used today, are irritant and even toxic; therefore, there is much interest in finding ways to formulate new types of safe and cost-effective biocidal materials, either natural or synthetic. Nanosize inorganic materials such as metals and semiconductors can cause denaturation of proteins present in bacterial cell walls during their antibiotic action (Behera *et al.*, 2012).

There are reports on antimicrobial activities of nanoparticles such as Ag, Au, MgO, CuO, Al, TiO₂, etc. that are effective against different drug resistant bacteria, viral and fungal strains (Rai and Bai, 2011). It was also reported the as synthesized nano-size materials including ZnS, Ag-N co-doped ZnS, Fe₂O₃ and ZnS/Fe₂O₃ composite have been tested for their antimicrobial activity against Gram positive (*Staphylococcus aureus* and *Streptococcus*) and Gram negative (*Pseudomonas aeruginosa* and *Escherichia coli*) bacteria (Yadav *et al.*, 2014). The test bacterial strains were streaked on nutrient agar in sterile Petri-dish. Using a micropipette, 10, 20 and 30 µl of 5 mg/mL of the nanomaterials, dispersed in water, were impregnated, separately, on paper discs, each of 5 mm diameters. The antimicrobial activities of the synthesized nanomaterials were evaluated in terms of magnitude of the measured inhibition zone after incubating at 37⁰C for 24 h.

In this present work, nano-size ZnS, CdS, NiS, ZnS/CdS, ZnS/NiS and ternary mixed metal sulfides (ZnS/CdS/NiS) nano composite was prepared by precipitation methods and characterized using XRD and Uv-Vis techniques. The as-synthesized nanomaterials were tested for their antimicrobial activity against Gram positive (*Staphylococcus aureus* and *Streptococcus*) and Gram negative (*Pseudomonas aeruginosa* and *Escherichia coli*) bacteria using paper disc diffusion technique.

Objective of the study

General Objective

- To evaluate the antimicrobial activities of ZnS/CdS/NiS nanocomposite prepared by precipitation method.

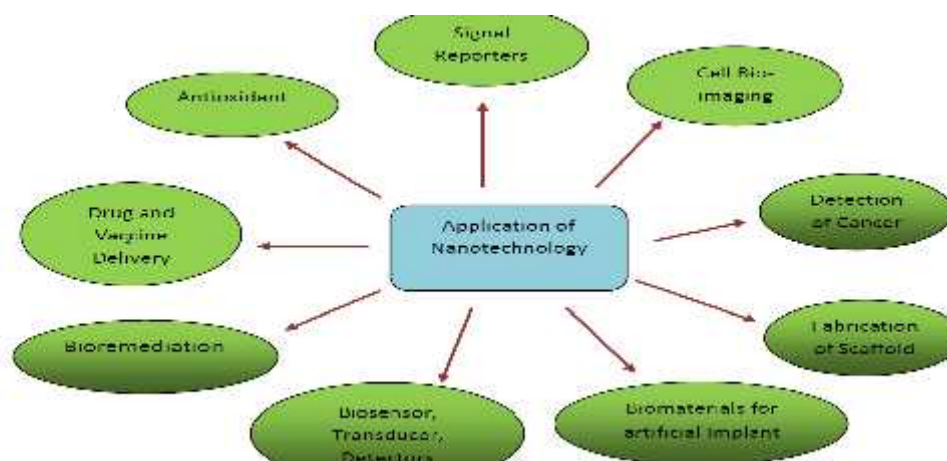
Specific objectives

- Synthesis of ZnS, CdS and NiS nanoparticles as well as the binary ZnS/CdS, ZnS/NiS and ternary mixed metal sulfides (ZnS/CdS/NiS) nanocomposite by precipitation method.
- Characterization of the as-synthesized nanomaterials using X-ray diffraction (XRD) and Uv-Vis spectroscopic techniques.
- Screening of the antimicrobial activities of as-synthesized nanomaterials against some selected bacterial species using the paper disc diffusion technique.

2. REVIEW OF RELATED LITERATURE

2.1. Applications and Uses of Nanotechnology

Nanoscience and nanotechnology have been an interesting field of research and gained much importance from last two decades. In layman terms “The study of properties of materials at nanoscale is termed as nanoscience, whereas the fabrication and application of the nanostructures are termed as nanotechnology”. Nanoparticles are the smallest of the microscopic particles or ultrafine particles which is having size in the range of 1-100 nm (Saxena *et al.*, 2010). Nanoscale dimensions of these particles give them high surface area to volume ratio that contribute to enhanced chemical activity, high surface plasmon resonance (SPR), enhanced Rayleigh scattering and surface enhanced Raman Scattering than compared their bulk material .The applications of nanoparticles are various such as signal reporters to detect various biomolecules in immunoassay, as flurophzore in fluorescence in situ hybridization (FISH) (Du, 2005), cell bio imaging, an antioxidant to remove free radicals from patient blood stream, delivering vaccines and drugs (Gupta and Sharma, 2011), treating infectious diseases, detection of cancer, fabrication of scaffolds and also more importantly in bioremediation .

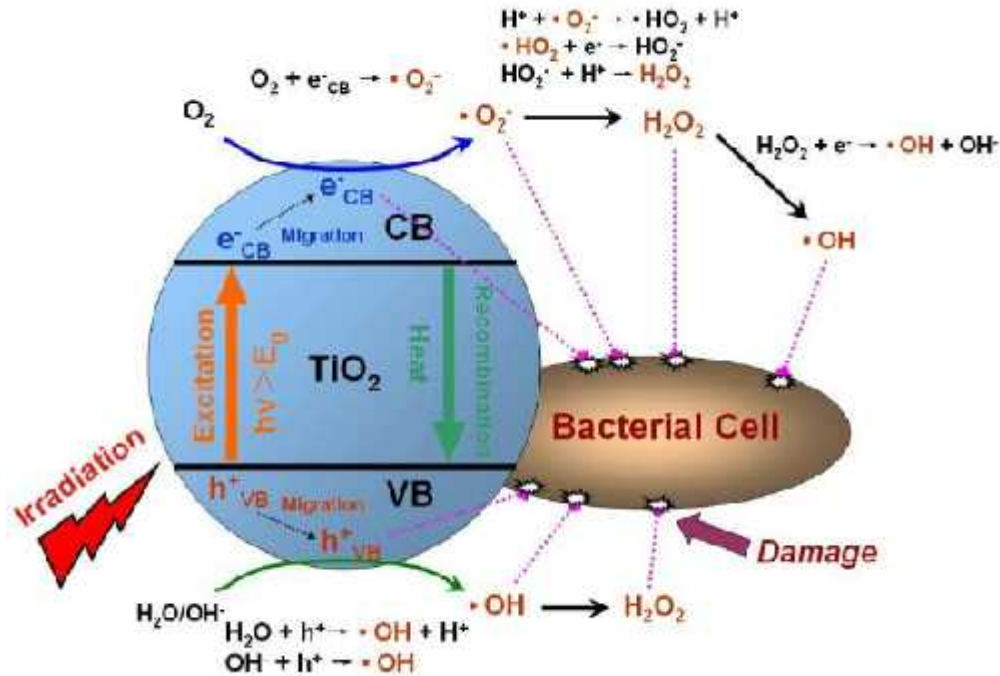


Scheme for different applications of nanotechnology

2.2. Applications and Properties of Nanoparticles

The dimension of matter important in nanoscience and nanotechnology is typically on the 0.2 to 100 nm scale (nanoscale). The properties of materials change as their size approaches the nanoscale. Further, the percentage of atoms at the surface of a material becomes more significant (Eustis and El-Sayed, 2006). Bulk materials possess relatively constant physical properties regardless of their size, but at the nanoscale this is often not the case. As the material becomes smaller the percentage of atoms at the surface increases relative to the total number of atoms of the material bulk. This can lead to unexpected properties of nanoparticles which are partly due to the surface of the material dominating over the bulk properties. At this scale, the surface-to-volume ratios of materials become large and their electronic energy states become discrete, leading to unique electronic, optical, magnetic, and mechanical properties of the nanomaterials. In general, as the size of inorganic and organic materials decreases towards the nanoscale, their optical and electronic properties largely varies from the bulk material at the atomic/molecular levels and is size and shape dependent (Gupta and Sharma, 2007). The various size dependent properties that can be observed are quantum confinement in semi-conductor particles, surface plasmon resonance in noble metal particles and super paramagnetism in magnetic materials. Thus, the crystallographic surface structure and the large surface to volume ratio make the nanoparticles exhibit remarkable properties. Moreover, the increased catalytic activity due to morphologies with highly active facets and the tailoring of its synthesis as per the requirement makes the nanoparticles an attractive tool to solve various technological problems (Jamieson *et al.*, 2007).

There are many reports on antimicrobial activities of nanoparticles such as Ag, Au, MgO, CuO, Al, TiO₂, etc. that is effective against different drug resistant bacteria, viral and fungal strains (Rai and Bai, 2011). Nano size inorganic materials such as metals and semiconductors can cause denaturation of proteins present in bacterial cell walls during their antibiotic action (Behera *et al.*, 2012). The scheme below shows the mechanism how TiO₂ nanoparticles damage bacterial cell walls.



2.3. Methods of Synthesis of Metal Sulfide and Mixed Metal Sulfide

Conventionally, transition metal sulphides have been prepared by numerous techniques, including chemical vapour transport, solid state reaction, and solution precipitation in aqueous and organic solutions. Transition metal sulphides show a variety of unusual structural and electronic properties which lead to important technical applications. Almost all transition metals starting from first group react with sulphur to form sulphides (Bither *et al.*, 1968)

Controlled synthesis of monodispersed inorganic nanocrystals with different sizes and shapes has attracted a great deal of attention in both fundamental research and technical application in recent years (Sun *et al.*, 2000). Especially, metal sulphide nanocrystals have been intensively pursued because of their unique size-dependent optical and electronic properties that are different from their bulk counterparts as well as their promising applications in solar cells, catalyses, light-emitting diodes, and biological detection devices (Huynhet *et al.*, 2002; Coe *et al.*, 2002). Metal sulphide nanocrystals with various shapes have been synthesized by different methods, such as, microwave irradiation, hydrothermal synthesis and ultrasonic irradiation. These methods are convenient and may lead to nanocrystals with controlled morphology. However, as prepared nanocrystals can grow continuously at a low temperature via coarsening

or epitaxial attachment because of the absence of strong repelling interactions between the particles resulting in the poor stability of the colloidal solution and thus affecting the optical and other physical properties of the nanocrystals (Cozzoli *et al.*, 2005).

Some transition metal sulphides can be prepared by a straight forward synthetic route to nanocrystallites metal sulphide such as zinc, cadmium, cobalt and nickel sulphides through metal salts and sulphur sources under the hydrothermal treatment in the ethylenediamine solution. Diammonium sulphide and thiourea have been used as sulphur sources and ZnCl_2 , $\text{CdCl}_2 \cdot 2.5\text{H}_2\text{O}$, $\text{CoCl}_2 \cdot 6\text{H}_2\text{O}$ and $\text{NiCl}_2 \cdot 6\text{H}_2\text{O}$ for respective metals (Wang *et al.*, 2005). Denga *et al* also reported the preparation of zinc, cadmium, nickel, cobalt and copper sulphide microspheres by hydrothermal methods. The method involves the precipitation of M^{2+} ($\text{M} = \text{Zn}, \text{Cd}, \text{Ni}, \text{Co}, \text{Cu}$) and $\text{S}_2\text{O}_3^{2-}$ with consequent hydrothermal treatment at 180°C for 10 h. A typical process involves the formation of equimolar solution of $\text{Na}_2\text{S}_2\text{O}_3$ and corresponding metal nitrate in distilled water. It is then mixed together in a 50 mL Teflon-lined autoclave and maintained at 180°C for 10 h. After the reaction was completed, the insoluble products were filtered, washed with water, ethanol and dried at 50°C for several hours (Denga *et al.*, 2006).

The CdS/ZnS core-shell structure was synthesized by seed growth method. The reaction matrix employed was consisted of AR grade ZnSO_4 , $(\text{NH}_4)_2\text{SO}_4$ and thiourea in 1:1.5:1.5 molar ratios. Zinc sulphatedehydrate, and ammonium sulphate were mixed in 50 mL of distilled water. Ammonia was added to it until the formation of clear metallic complexes. The pH was kept at 9.5. After this processes prepared CdS solution was added (2.5 mL) of as mentioned in CdS synthesis as above. Then thiourea was dissolving in 50 mL of prepared solution. After that a 5% solution of 2-mercaptoethenaoil was added in solution for passivation then continuously stirred for 5 h. When the reaction was completed, CdS/ZnS core-shell nanocrystals was obtained (Hitanshu *et al.*, 2014). In some cases, the oxide is reacted with different sulphur sources such as thioglycolic acid, thiourea, or elemental sulphur to produce the corresponding sulphide. For example, ZnO/ZnS, $\text{SnO}_2/\text{SnS}_2$, $\text{MnO}_2/\text{MnS}_2$ core-shell nanostructures, and nanotubes of ZnS and SnS_2 were formed when the corresponding oxide was reacted with Na_2S and thioglycolic acid (Zhang *et al.*, 2005)

2.4. Applications and properties of Metal Sulfides (II-VI) Semiconductors

2.4.1. Zinc Sulfide (ZnS)

In the past decade, II-VI semiconductor nanoparticles attract much attention because of their size-dependent (and thus tunable) photo- and electro- luminescence properties and promising applications in optoelectronics. Among the family of II–VI semiconductors, ZnS, CdS, CdTe etc. are the foremost candidates because of their favorable electronic and Optical properties for optoelectronic applications (Tittel *et al.*, 2009). Among those ZnS is a commercially important II–VI semiconductor having a wide optical band gap, rendering it a very attractive material for optical application especially in nanocrystalline form. ZnS can have two different crystal structures (zinc blende and wurtzite), both of which have the same band gap energy (3.68 eV) and the direct band structure. ZnS has been used for the cathode ray tube, the field emission display, and the scintillator as one of the most frequently used phosphors (Ghrayeb *et al.*, 1997)

2.4.2. Cadmium Sulfide (CdS)

Cadmium sulfide is an important semiconducting material used for different applications in optoelectronics such as nonlinear optics, flat panel displays, light emitting diodes, lasers, and thin film transistors, etc. Semiconducting cadmium sulphide has been widely used as a yellow pigment and, in recent years, has been actively studied for application as a photo catalyst for generation of hydrogen from water, as a window layer material for CdS/CdTe solar cells, and for various optoelectronic devices. This is apparently due to the fact that its band gap is appropriate for absorption of visible light, and it's detailed photochemical or photoelectron chemical activity varies with such physical properties as crystalline phase, size, and morphology of the cadmium sulphide particles (kanasal, 2007).

Textile industries produce large volume of colored dye effluents which are toxic and non biodegradable. These dyes create severe environmental pollution problems by releasing toxic and potential carcinogenic substances into the aqueous phase. Cadmium sulphide is very active photo catalyst for the complete destruction of these dyes (Kansal, 2007). Semiconductor-assisted splitting of water under solar radiation is considered as a clean, renewable and abundant source of hydrogen fuel. Among various photo catalysts developed for this purpose, cadmium

sulphide continues to be a favoured material because of its ideal band gap (2.3 eV) that corresponds well with the electromagnetic spectrum of solar radiation (Pooja, 2007). Semiconductor nanocrystals of cadmium sulphide have received considerable attention because of their intrinsic properties of a narrow band gap, good chemical stability and ready preparation, and their technological applications, ranging from microelectronics to non-linear optics, optoelectronics, catalysis, optical windows for solar cell and photo-electrochemistry.

Electronically conducting materials that contain sulphur as part of their chemical composition are excellent electro-catalysts for both anodic and cathodic reactions for the sulphide/polysulphide redox couple. The electrochemistry of sulphide/polysulphide couple becomes more attractive due to the development of energy conversion and storage applications, photo-electrochemical energy conversion, electrodes in the solar cells and Li-sulphur batteries. Sulphide/polysulphide couple is an understood material for an aqueous electrochemical storage device (Tittel *et al.*, 2009). Semiconductor quantum dots, because of their large ratio of surface atoms and the three dimensional quantum confinement of excitons, are of great interest for people engaged in fundamental and applied research. Among various semiconductor materials, cadmium sulphide has been extensively investigated and used as an important direct-band semiconductor, for the photoelectric conversion in solar cells, and other optical devices based on its nonlinear properties (Lou, 2007).

2.4.3. Nickel Sulfide (NiS)

Transition metal sulfide nanostructures have been the focus of considerable interest due to their unique optical and electrical properties and wide variety of potential applications in devices such as nonlinear optical devices, semiconductor, electroluminescence devices, industrial catalysts, solar energy conversion devices, fluorescence devices and even light emitting diodes for flat-panel displays, superconductor etc (Klimov *et al.*, 2000). Transition metal (TM) sulfides exhibit interesting optical, electronic, thermoelectric and photoelectric properties. Nickel sulfide (NiS) is an important member of this large family of transition metal sulfides, finds use as a potential cathode material for the rechargeable lithium battery, as a catalyst in the degradation of organic dyes and in magnetic devices (Klimov *et al.*, 2000). Owing to the tremendous technological importance, different synthesis routes have been tried for the synthesis of

nanoparticles of NiS. Some of the techniques, which have been used for the preparation of nanoparticles include solvothermal process, UV irradiation, sol-gel method, laser ablation within copolymer and colloidal microemulsion etc. The chemical precipitation method is one of the important methods for the synthesis of nanoparticles.

2.5. Antimicrobial activities of Metal sulfide Nanomaterials

2.5.1 Zinc Sulfide (ZnS)

The nanoparticles possess unique physico-chemical, optical and biological properties which can be manipulated suitably for desired applications. Moreover, as the biological processes also occur at the nanoscale and due to their amenability to biological functionalization, the nanoparticles are finding important applications in the field of medicine (Parak *et al.*, 2003). The nanoparticles are broadly grouped into organic and inorganic nanoparticles. The latter have gained significant importance due to their ability to withstand adverse processing conditions (Whitesides, 2003). Currently, the metallic nanoparticles are thoroughly being explored and extensively investigated as potential antimicrobials. The antimicrobial activity of the nanoparticles is known to be a function of the surface area in contact with the microorganisms. The small size and the high surface to volume ratio *i.e.*, large surface area of the nanoparticles enhances their interaction with the microbes to carry out a broad range of probable antimicrobial activities. Metal nanoparticles with antimicrobial activity when embedded and coated on to surfaces can find immense applications in water treatment, synthetic textiles, biomedical and surgical devices, food processing and packaging (Gutierrez *et al.*, 2010). Moreover, the composites prepared using metal nanoparticles and polymers can find better utilization due to the enhanced antimicrobial activity.

Yadav *et al.*, (2014), reported that the anti-microbial activity of as synthesized nano-size ZnS, Ag-N co-doped ZnS, Fe₂O₃ and ZnS/Fe₂O₃ composite against gram positive (*Staphylococcus aureus* and *Streptococcus*) and gram negative (*Pseudomonas aeruginosa* and *Escherichia coli*) bacteria. Doping of Ag and N into ZnS showed cumulative effect on enhancing the antimicrobial activity of ZnS. Undoped as well as Ag and N co-doped ZnS exhibited higher activity against Gram positive bacteria than Gram negative bacteria. Antimicrobial activity of Ag-N co-doped ZnS was also compared with the activity of two

commercially available antibiotics Gentamycin and Azithromycin. Compositing of Fe₂O₃ with ZnS showed antagonistic effect towards the antimicrobial activity of the later.

A micropipette was used to measure the different volume which was 10, 20 and 30 µl 5 mg/ml of the nanomaterial, dispersed in water, and impregnated separately on paper discs, each of 5 mm diameters. Then evaluated the antimicrobial activity of the synthesized nanomaterial in terms of magnitude of the measured inhibition zone after incubating at 37 °C for 24 h.

2.5.2. Cadmium Sulfide (CdS)

Popova *et al.*, (2012) reported antimicrobial susceptibility testing of CdS nanoparticles (pure and Cu doped) against bacteria *Staphylococcus aureus*, *Salmonella typhimurium*, *Pseudomonas aeruginosa*, *E. coli* and *Klebsiella pneumoniae*. Cu doped CdS nanoparticles were more effective with MIC range 0.078-0.52 mg/ml. as compared to pure CdS nanoparticles with MIC range 0.15- 0.83 mg/ml. This indicates the fact that dopant was interfering with the active principle as the MIC values are smaller in Cu doped CdS nps as compared to pure CdS nps for different groups of bacteria. The highest activity was observed against *Staphylococcus aureus* with MIC 0.078 mg/ml. The bacteria least susceptible was *E. coli* with MIC 0.83mg/ml. The antimicrobial study also showed that standard isolates were more susceptible than clinical isolates. The effect is more pronounced in case of Gram positive bacteria as compared to Gram negative bacteria. CdS nanoparticles showed broad spectrum activity. (Popova *et al.*, 2012). There is one report about the antibacterial activity of CdS nanoparticles on *E. coli* (Sarita, 2010).

2.5.3. Nickel Sulfide (NiS)

The *in vitro* effect of four nickel complexes with ligands containing the anti pyrine moiety N,N' bis(4-antipyrylmethyl)-piperazine (BAMP) and N,N'-tetra-(antipyryl-1-methyl)-1,2-diaminoethane against 33 pathogenic bacterial strains, as well as control ones, was examined. The antifungal activity of the complexes against four *Candida* spp. was established too. Two routine methods were used: of Bauer-Kirby and the determination of minimum inhibitory concentrations. The compounds Ni (TAMEN)(NCS)₂ and Ni(TAMEN)(ClO₄)₂ manifested good antibacterial activity *in vitro* against the tested bacteria, especially towards the Gram-

positive strains, as well as against *K. pneumoniae* and *P. aeruginosa*. Among all tested microorganisms, the sensitivity of the strains of *E. coli* to the examined complexes proved most weak. *Candida* spp. showed high sensitivity to Ni(TAMEN)(NCS)₂ and Ni(TAMEN)(ClO₄)₂ too and weaker to Ni₂(BAMP)(Cl)₄ and Ni₂(BAMP)(Ac) (Popova1 *et al*, 2012)

Nickel is one of the metals with antimicrobial properties. Its ions can penetrate in microbial cells and kill them mainly by inactivating their enzymes (Chohan, 2000). Many investigations show that different nickel (II) complexes manifest antimicrobial action (Rao and Reddy, 1990; Chohan *et al.*, 2002). Dependence of the inhibitory activity of the metal ions from the chelate geometry and thermal stability of the metal complexes has been established (Kamalakannan and Venkappayya, 2002). Appreciable antimicrobial activity in comparison with the ligands has been proved in some nickel compounds (Shivankar and Takkar, 2003). Blasco *et al.*, 1996 established that in complexation with sulfanilamide derivatives, nickel (II) and other metal ions enhance their inhibitory activity *in vitro* against such important relative pathogens as *E. coli* and *S. aureus*.

3. MATERIALS AND METHODS

3.1. Experimental Site

Synthesis of the single metal sulfides, ZnS, CdS, the binary metal sulfides, ZnS/CdS and ZnS/NiS as well as the ternary mixed metal sulfide, ZnS/CdS/NiS nanomaterials and Uv-Vis studies were carried out at Chemistry Department Instrumental Laboratory, Haramaya University. Antimicrobial screening of the nanoparticles and nanocomposite was performed by Paper Disc Diffusion technique against Gram positive (*Staphylococcus aureus* and *Streptococcus*) as well as Gram negative (*Pseudomonas aeruginosa* and *Escherichia Coli*) bacteria at the Department of Plant Science College of Agriculture, Haramaya University. The synthesized samples were characterized by XRD technique at the Department of Material science Engineering, Adama Science and Technology University (ASTU).

3.2. Materials and Apparatus

3.2.1. Chemicals and Reagents

In this work Zinc nitrate hexahydrate $Zn(NO_3)_2 \cdot 6H_2O$, $M_w=297.47$ g/mol), sodium sulfide nonahydrate ($Na_2S \cdot 9H_2O$, $M=250.04$ g/mol, cadmium nitrate tetrahydrate ($Cd(NO_3)_2 \cdot 4H_2O$), $M_w=308.4$ g/mol), Nickel nitrate tetrahydrate ($Ni(NO_3)_2 \cdot 4H_2O$, $M_w= 254.72$ g/mol), Glucose ($C_6H_{12}O_6$), $M_w=180.16$ g/mol), hydrochloric acid (HCl), ethanol (C_2H_5OH) and deionized water, were used.

3.2.2. Apparatus and Instruments

Instruments and apparatus used for synthesis and characterization of nanomaterials includes, Uv-Visible spectroscopy, XRD, oven, graphite furnace, electronic balance, magnetic stirrer, centrifuge, measuring cylinder, ceramic crucibles, volumetric flasks, pipettes, test tubes, glass rod, Petri-dishes, nutrient agar plates, etc.

3.3. Synthesis Methods

3.3.1. Synthesis of ZnS Nanoparticles

A measured volume 100 mL of 1.0 M aqueous solution of Sodium sulfide nonahydrate ($\text{Na}_2\text{S} \cdot 9\text{H}_2\text{O}$, MW = 250.04 g/mol) was added drop-wise, at 70°C to equal volume 100 mL of 1.0 M aqueous solution of Zinc nitrate hexahydrate ($\text{Zn}(\text{NO}_3)_2 \cdot 6\text{H}_2\text{O}$, MW=297.47 g/mol) with simultaneous magnetic stirring for 15 h to get a white suspension. To the suspend thus obtained, 100 mL of glucose ($\text{C}_6\text{H}_{12}\text{O}_6$, MW = 180.16 g/mol) solution was added drop-wise and the resultant mixture was incubated at 70°C for 6 h and centrifuged at 2000 rpm for 15 min and the precipitate so obtained was filtered off and dried at 50°C for 4 h. The well dried solid was then crushed to a fine powder and labeled as ZnS nanomaterial (Senapati *et al.*, 2013).

3.3.2. Synthesis of CdS Nanoparticles

A measured volume of 100 mL of 0.1 M aqueous solution of sodium sulfide nonahydrate ($\text{Na}_2\text{S} \cdot 9\text{H}_2\text{O}$) was added drop-wise at 80°C to 100 mL of 0.1 M aqueous solution of cadmium nitrate tetrahydrate ($\text{Cd}(\text{NO}_3)_2 \cdot 4\text{H}_2\text{O}$) with continuous stirring for 15 h using magnetic stirrer. Then 100 mL of 1.0 M ethanol was added drop-wise followed by addition of 15 mL of deionized water drop by drop. After wards, the mixture was cooled at room temperature and filtered. Then the yellow precipitate so obtained was dried in an oven at 80°C for 24 h and then calcined at 300°C for 2 h. Finally, the solid sample was ground in an agate mortar and labeled as CdS nanomaterial (Senapati *et al.*, 2013).

3.3.3. Synthesis of NiS Nanoparticles

A measured volume of 100 mL of 0.1 M aqueous solution of sodium sulfide nonahydrate ($\text{Na}_2\text{S} \cdot 9\text{H}_2\text{O}$) was added drop-wise at 80°C to 100 mL of 0.1 M aqueous solution of nickel nitrate tetrahydrate ($\text{Ni}(\text{NO}_3)_2 \cdot 4\text{H}_2\text{O}$) with continuous stirring for 5 h using magnetic stirrer. After the reaction was completed, the insoluble black precipitate was filtered, washed with water, ethanol and dried at 50°C for several h and then calcined at 250°C for 2 h and ground into powder and then labeled as NiS nanomaterial (Denga *et al.*, 2006).

3.3.4. Synthesis of ZnS/CdS Nanocomposite

The Binary nanocomposite ZnS/CdS was prepared by mixing equal volume of 0.1 M aqueous solutions of sodium sulfide nonahydrate ($\text{Na}_2\text{S} \cdot 9\text{H}_2\text{O}$) and zinc nitrate hexahydrate ($\text{Zn}(\text{NO}_3)_2 \cdot 6\text{H}_2\text{O}$) to serve as ZnS precursor; and sodium sulfide nonahydrate ($\text{Na}_2\text{S} \cdot 9\text{H}_2\text{O}$) and Cadmium nitrate tetrahydrate ($\text{Cd}(\text{NO}_3)_2 \cdot 4\text{H}_2\text{O}$) to serve as CdS precursor and these two sulfides make up a composition of (0.8 : 0.2) by mass of ZnS : CdS, respectively. After 3 h of stirring the mixture yielded a yellow precipitate which was then collected and washed several times with ethanol, and kept to dry in an oven at 60°C and calcined at 300°C for 2 h and finally crushed into fine powder and labeled as ZnS/CdS nanocomposite (Hitanshu *et al.*, 2014).

3.3.5. Synthesis of ZnS/NiS Nanocomposite

Likewise the binary nanocomposite, ZnS/NiS was prepared by mixing equal volume of 0.1 M aqueous solutions of sodium sulfide nonahydrate ($\text{Na}_2\text{S} \cdot 9\text{H}_2\text{O}$) and zinc nitrate hexahydrate ($\text{Zn}(\text{NO}_3)_2 \cdot 6\text{H}_2\text{O}$) to serve as ZnS precursor; and sodium sulfide nonahydrate ($\text{Na}_2\text{S} \cdot 9\text{H}_2\text{O}$) and Nickel nitrate tetrahydrate ($\text{Ni}(\text{NO}_3)_2 \cdot 4\text{H}_2\text{O}$) to serve as NiS precursor and these two sulfides make up a composition of 0.8 : 0.2 by mass of ZnS : NiS respectively. After 3 h of stirring the mixture yielded a black precipitate which was then collected and washed several times with ethanol and kept to dry in an oven at 60°C and then calcined at 300°C for 2 h and finally crushed in to fine powder and labeled as ZnS/NiS nanocomposite .

3.3.6. Synthesis of ZnS/CdS/NiS Nanocomposites.

The ternary nanocomposite ZnS/CdS/NiS was finally prepared by mixing equal volume of 0.1 M aqueous solutions of sodium sulfide nonahydrate ($\text{Na}_2\text{S} \cdot 9\text{H}_2\text{O}$) and zinc nitrate hexahydrate ($\text{Zn}(\text{NO}_3)_2 \cdot 6\text{H}_2\text{O}$), to serve as ZnS precursor; and sodium sulfide nonahydrate ($\text{Na}_2\text{S} \cdot 9\text{H}_2\text{O}$) and Cadmium nitrate tetrahydrate ($\text{Cd}(\text{NO}_3)_2 \cdot 4\text{H}_2\text{O}$), to serve as CdS precursor, and sodium sulfide nonahydrate ($\text{Na}_2\text{S} \cdot 9\text{H}_2\text{O}$) and Nickel nitrate tetrahydrate ($\text{Ni}(\text{NO}_3)_2 \cdot 4\text{H}_2\text{O}$) to serve as NiS precursor. These three sulfides give a composition of (0.7: 0.1: 0.2) by mass of ZnS : CdS : NiS, respectively. After 3 h of stirring the mixture yielded a black precipitate which was then collected and washed several times with ethanol and after drying it in an oven at 60°C it was

then calcined at 300⁰ C for 2 h and finally crushed in to fine powder and labeled as ZnS/CdS/NiS nanocomposite .

3.4. Characterization Methods

3.4.1. Analysis of Uv-Vis Diffuse Reflectance Absorption Spectra

The Uv-Vis Diffuse Reflectance Absorption Spectra of the nanoparticles and nanocomposite was recorded for determining their respective absorption edges and maximum wave lengths. Band gaps energy (E_g) of the as-synthesized nanoparticles were obtained from the Tauc plot. Tauc plot is one method of determining the optical band gap in semiconductors. The square root of the product of the absorption coefficient and photon energy is plotted versus photon energy. The curve should have a section of straight line. If extended to the X-axis, the X-intercept of this line gives the optical band gap (Senapati *et al.*, 2013).

Using this curve the optical band gap is determined based on Tauc's equation as given below

$$h = A(h - E_g)^n$$

Where, A is a constant, h is photon energy, E_g is the allowed energy gap, is absorption coefficient, $n = 1/2$ for allowed direct transition and $n = 2$ for allowed indirect transition.

3.4.2. X-ray Diffraction Measurements

For determining the crystallite nature and size of the as-synthesized photocatalyst materials, their X-ray diffraction (XRD) patterns were recorded using a diffractometer equipped with a Cu target K radiation ($\lambda = 1.5405 \text{ \AA}$) source. The measurement was made at room temperature using accelerating voltage and the applied current of 40 kV and 30 mA, respectively, over 2 range of 10^o to 80^o.

The average crystallite sizes of the as synthesized material were calculated using the Debeye–Scherrer formula (Mamta Yadav *et al.*, 2014). $D = (K \lambda) / (\cos \theta)$, Where, D is the average particle size, λ is the wavelength (0.15406 nm) of X-ray; $\Delta 2\theta$ is the full width at half-maxima (FWHM) of the diffraction peak of highest intensity and θ is the incident angle of X-ray; K is the geometric factor equal to 0.94.

3.5. Antimicrobial Screening of the as- Synthesized Nanoparticles

Antimicrobial screening tests were conducted against four different important bacteria, Gram positive (*Staphylococcus aureus* and *Streptococcus*) and Gram negative (*Pseudomonas aeruginosa* and *Escherichia coli*) bacteria using paper disc diffusion technique (Gebru *et al.*, 2003). The bacterial strains were streaked on nutrient agar in sterile Petri dishes. chlroamphinicol, a standard antibiotic drug was used as a reference in bacteriacidal studies. From the inhibition zone data correlations of structures with antimicrobial activity of compounds were critically examined.

3.5.1. Preparation of Media

Bacteria (*Staphylococcus aureus* and *Streptococcus*) and (*Pseudomonas aeruginosa* and *Escherichia coli*) were transferred from the culture and then streaked on Mueller Hinton Agar (MHA) plate and incubated for 24h at 37°C. The bacteria were transferred to the autoclaved MHA and cooled at about 45°C in water bath and mixed vigorous by swirling of flasks. The medium was poured to sterilize Petri-dishes. Lastly, the media containing spore suspension were poured to sterilized plates, solidified and used for the bio tests.

3.5.2. Procedure for Anti-microbial Activity Test.

A 6 mm diameter paper disc of Whatmann No.1 filter paper was pierced with office puncture and the disc was sterilized in oven at 180°C for 1h and a 30 µl of solution of nanoparticles were pipetted on the discs. Finally, the samples were transferred with sterile forces onto the impregnated disc paper onto nutrient agar plate seeded with bacteria and incubated at 37°C for 24 h.

4. RESULTS AND DISCUSSION

4.1. Characterization of the as-Synthesized Nanomaterials

4.1.1. Analysis of Uv-Vis Diffuse Reflectance Absorption Spectra

Many semiconductors with good photocatalytic properties have band gaps that are too large for absorption of visible light. Thus, they have low efficiencies under sunlight. One best example is ZnS with band gap of 3.82 eV. Compositing of such a semiconductor is one strategy for reducing the band gap energy and thus increase its visible-light absorption efficiency (Huang, *et al.*, 2013)

The study of optical absorption is important to understand the behavior of semiconductor nanoparticles. A fundamental property of semiconductors is the band gap-the energy separation between the filled valence band and the empty conduction band. Optical excitation of electrons across the band gap is strongly allowed, producing an abrupt increase in absorption at the wavelength corresponding to the band gap energy (E_g). From the absorption edges of ZnS, CdS, NiS, ZnS/CdS, ZnS/NiS and ZnS/CdS/NiS the band gap energies (E_g) of each as-synthesized nanomaterial was obtained from Tauc plot (See figure1).

A Tauc plot is one method of determining the optical band gap in semiconductors in which the square root of the product of the absorption coefficient and photon energy is plotted versus photon energy. The curve should have a section of straight line, and if this line is extended to the X-axis, the X-intercept of this line gives the optical band gap (Senapati *et al.*, 2013).

Using this curve the optical band gap is determined based on Tauc's equation as given below:

$$h = A(h - E_g)^n$$

Where, A is a constant, h is photon energy, is absorption coefficient, E_g is the allowed energy gap, $n = 1/2$ for allowed direct transition and $n = 2$ for allowed indirect transition

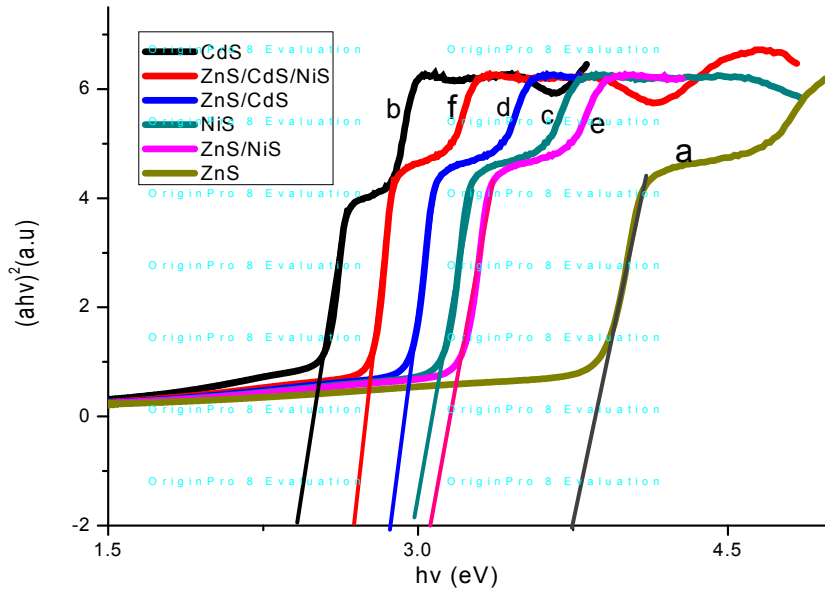


Figure 1. Tauc plots (a) ZnS, (b) CdS, (c) NiS, (d) ZnS/CdS, (e) ZnS/NiS and (f) ZnS/CdS/NiS nanomaterials.

At room temperature UV-Vis absorption spectrum of the ZnS, CdS, NiS, ZnS/CdS, ZnS/NiS and ZnS/CdS/NiS nanomaterials were measured in the wavelength range of 200-700 nm. From the data of absorbance versus wavelength of the as-synthesized nanomaterials the band gap energies (E_g) were obtained using Tauc plot.

Accordingly as indicated the plot 1(a), the optical band gap energy of (E_g) of ZnS was found to be 3.76 eV which corresponds to the absorption edge of 330 nm. This value when compared with that of the bulk ZnS as reported in the literature as 3.65 eV (340 nm), the absorption spectrum of the as synthesized ZnS showed a blue shift i.e. towards the high energy side indicating that the ZnS nanoparticles were quantum-confined. This result is in good agreement with the work of Olumide *et al.*, (2014), where the band gap of ZnS were reported as 3.82 eV and 3.65 eV for nanosized and the bulk samples, respectively.

Similarly, the plot 1(b) shows the optical band gap energy (E_g) of the as-synthesized CdS was found to be 2.49 eV which corresponds to the absorption edge of 497 nm. This value when compared with that of the bulk CdS, there is also blue shift (towards high energy), indicating that the CdS nanoparticles were quantum-confined as well. This result is also in agreement with an earlier literature report on similar work (Alivisatos, 1996).

The plot 1(c) represents the optical band gap energy (E_g) of NiS nanoparticles, which was found to be 3.11 eV and corresponds to the absorption edge of 398 nm. When compared with the bulk NiS (0.4 eV), the value reported by Attay, (2002), we can observe here also the band gap of the samples highly blue shifted towards higher energy, indicating that the NiS nanoparticles were quantum-confined. This value is also in good agreement with that reported by Alin *et al.*, (2015), for a NiS sample as 2.8 eV at (1000 C⁰).

The plot 1(d) on the other hand, provides the optical band gap energy (E_g) of 2.88 eV for the binary ZnS/CdS nanocomposite corresponding to absorption edge of (430 nm). When compared with the band gap of both CdS (2.49 eV) and ZnS (3.76 eV), the value obtained for binary sulfide nanocomposite lies within the expected value. This observation is in agreement with the work of *Hitanshu et al.*, (2014), where the reported band gap value of CdS/ZnS lies between the band gap values of CdS and ZnS. We can observe that the absorption edge of the ZnS/CdS nanocomposite shows a blue shift in the visible region with respect to that of CdS and redshift with that of ZnS. This could be attributed to the interfacial interaction between particles of ZnS and CdS.

Likewise, the plot 1(e) shows the absorption curve of the binary ZnS/NiS nanocomposite from which its band gap (E_g) was determined and to be 3.15 eV corresponding to the measured absorption edge of 393 nm. When compared with the band gap of the individual sulfides, NiS (3.11 eV) and ZnS (3.76 eV), the value obtained for the binary sulfide lies within the expected range. This observation is in agreement with the work of *Hitanshu et al.*, (2014), where by the observed absorption edge of the ZnS/NiS nanocomposite showed a slightly blue shift in the visible region with respect NiS (398 nm) and a red shift with that of ZnS (330 nm). By the same taken, these shifts could be attributed to the interfacial interaction between particles of ZnS and NiS.

Lastly, the plot labeled 1(f) represents the absorption curve of the ternary nanocomposite of the ZnS/CdS/NiS from which the band gap (E_g) was determined and found to be 2.77 eV (448 nm). This value actually lies in between the high energy value of ZnS (3.76 eV) and the lowest of CdS (2.49 eV). as it can be observed the absorption edge of the ZnS/CdS/NiS (448 nm) nanocomposite shows a relatively lower energy red shift compared to that of ZnS (330 nm).

This could be attributed to the interfacial interaction between particles of ZnS, CdS and NiS. Loading some CdS and NiS nanoparticles in to the host ZnS has consequently driven the band edge of the latter to the lower energy side and there by enhanced the photocatalytic activities of ZnS under visible-light.

4.1.2. Analysis of X-ray Diffraction Patterns of the Nanomaterials

The XRD patterns of the nanomaterials: ZnS, CdS, NiS, ZnS/CdS, ZnS/NiS and ZnS/CdS/NiS are shown in figures 2(a), (b), (c), (d), (e) and (f,) respectively, all of which were recorded over 2 range of 10° - 80° .

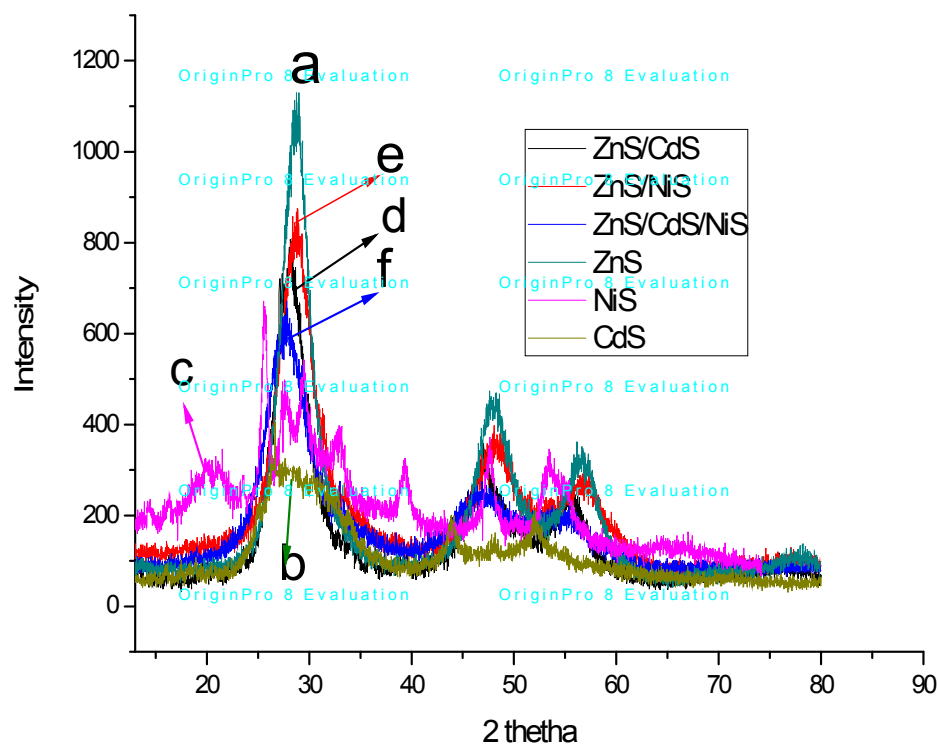


Figure 2. The XRD patterns of the as-synthesized nanomaterials: (a) ZnS, (b) CdS, (c) NiS, (d) ZnS/CdS, (e) ZnS/NiS and (f) ZnS/CdS/NiS.

Figure 2(a) represents the X-ray diffraction pattern of as-synthesized ZnS. Here three broad peaks were observed at 28.7° , 48.0° and 56.6° which correspond to the (111), (220) and (311) planes of cubic blend structure of ZnS respectively, which agree with the literature (JCPDS 05-0566), indicating that crystalline ZnS nanomaterials were successfully synthesized.

The average crystallite size was calculated using Debye-Scherrer formula, for the prominent (111) plane and found to be 2.5 nm. This value is in good agreement with value obtained by Shubhangi *et al.*, (2010).

Figure (2b) represents the X-ray diffraction pattern of as-synthesized CdS. The peaks appearing at 2 theta values of 26.6° , 43.9° , and 52.8° are due to diffraction by the (111), (220) and (311) planes of face centered cubic structure of CdS, respectively. This value is in good agreement with the value obtained by Nayereh Soltani *et al.*, (2012). The calculated crystallite size for the prominent (111) plane was found to be 5.3 nm.

Figure (2c) represents the X-ray diffraction pattern of as-synthesized NiS. Here five strong broad peaks were observed in the diffractogram at 31.5° , 35.2° , 45.5° , 53.45° and 60.1° , which correspond to the (100), (101), (102), (110) and (103) planes, respectively. This match well with hexagonal structure of NiS and agree with the literature (JCPDS file no: 01-075-0613). The presence of broad peaks in XRD implies the formation of nanoparticles. The calculated crystallite size for NiS was found to be 8.6 nm at the prominent diffraction angle of 31.5° .

Figure (2d) represents the X-ray diffraction patterns of synthesized ZnS/CdS. In this case also three broad peaks were observed in the diffractogram at 28° , 46.7° and 55.5° , which corresponding to the (111), (220) and (311) planes of cubic structures of ZnS (JCPDS 05-0566) respectively. No new additional diffraction peaks were observed this can be because of the peaks of ZnS were almost at same position of CdS, thus the cubic structure of CdS and that of ZnS peaks were overlapped together at a plane of (111), (220) and (311) and coexist as ZnS/CdS nanocomposite. This observation was in good agreement with the work of Sarmila Dutta *et al.*, (2012). The particle size of ZnS/CdS was calculated using Debye Scherrer formula and was found to be 2.6 nm at prominent the diffraction angle of 28.0° .

Figure (2e) represents the X-ray diffraction pattern of synthesized ZnS/NiS. Three broad peaks are observed in the diffractogram at 28.7° , 48.3° and 57.5° , which match well with (111), (220) and (311) planes of cubic blend structure of ZnS (JCPDS 05-0566) respectively. Strong ZnS crystalline phases appeared and no obvious diffraction peaks of NiS were observed, probably because the amount of NiS is too small and/or there was weak crystallization. The calculated

particle size of ZnS/NiS using Debye Scherrer formula and was found to be 2.8 nm at prominent the diffraction angle of 28.7° .

Figure (2f) represents the X-ray diffraction patterns of synthesized ZnS/CdS/NiS. Here also three broad peaks were observed in the diffractogram at around 28.13° , 48.3° and 55.3° which correspond to a planes (111), (220) and (311) and match well with cubicblende structure of ZnS (JCPDS 05-0566) respectively. Strong ZnS crystalline phases appeared due to diffraction peaks of cubic structures of CdS and ZnS overlapped at a plane of (111), (220) and (311), and no obvious diffraction peaks of NiS were observed, probably because the amount of NiS is too small and/or there was weak crystallization. The calculated crystallite size for ZnS/CdS/NiS was found to be 3.3 nm at the prominent diffraction angle of 28.13° . In all pattern no peaks corresponding to impurities were detected. The formation of sharp peaks indicates the crystalline nature of the materials. The increase in the peak width is the evidence of decrease of particle sizes.

Table 1. The crystallite sizes (D) of the as-synthesized nanomaterials.

Samples	2θ (degree)	(radian)	D (nm)	Band gap energy
ZnS	28.7°	0.059	2.5	3.76 eV
CdS	26.6°	0.0286	5.3	2.49 eV
NiS	31.5°	0.0175	8.6	3.11 eV
ZnS/CdS	28.18°	0.0576	2.6	2.88 eV
ZnS/NiS	28.7°	0.054	2.8	3.15 eV
ZnS/CdS/NiS	28.13°	0.0453	3.3	2.77 eV

4.2. Antimicrobial Activities of the As-synthesized Nanomaterials

Some of inhibition zone produced by the as synthesized antibiotic materials are shown below in figures 3 to 6.

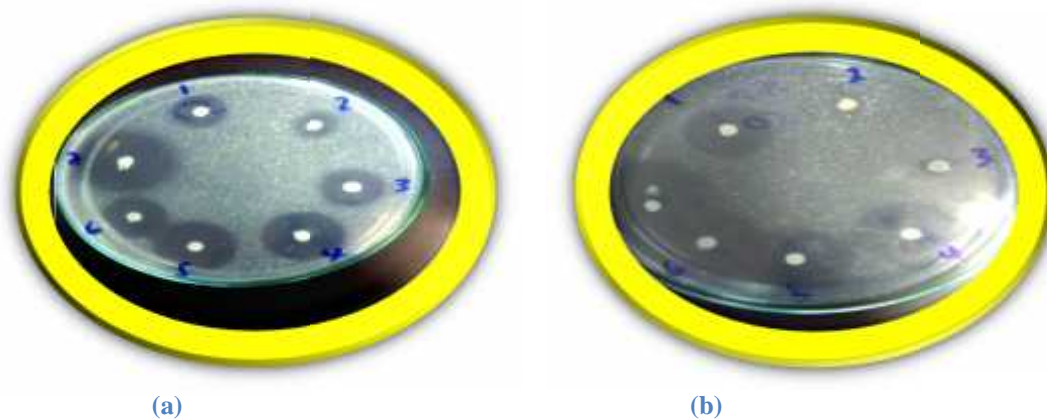


Figure 3 (a) and 3 (b). Inhibition zone of as synthesized NPs against *Staphylococcus aureus* bacteria at concentrations of 100 (a) and 150 (b) in $\mu\text{g/mL}$ respectively.

In this case (1, 2,3,4,5 and 6) represents as-synthesized nanomaterials such as ZnS, CdS, NiS, ZnS/CdS, ZnS/NiS, and ZnS/CdS/NiS respectively, where as 7 for commercially available Chloramphenicol.

Zone of inhibition (in mm) of the synthesized nanomaterials acting as antibiotics against the studied bacteria were presented in table 2. It was observed that the synthesized nanomaterials act as stronger antibiotics against Gram positive (*Staphylococcus aureus* and *Streptococcus*) bacteria than the Gram negative (*Pseudomonas aeruginosa* and *Escherichia coli*) bacteria. The attachment of CdS and NiS into ZnS to form ZnS/CdS/NiS nanocomposite showed a cumulative effect at improving the antimicrobial activity of ZnS. The binary nanocomposite also shows a better antimicrobial activities than the individual sulfides: ZnS, CdS and NiS nanoparticles. Order of antimicrobial activities of the ZnS/CdS/NiS NCs against the studied bacteria is: (*staphylococcus aureus*)> (*streptococcus*)> (*Escherichia coli*) > (*Pseudomonas aeruginosa*).

The minimum effective doze for each synthesized nanomaterial was found to be 150 $\mu\text{g/mL}$. This value indicates that as concentration increase, the antimicrobial activities of the as-synthesized nanomaterials against the selected bacteria increase. In general ZnS/CdS/NiS nanocompsite exhibited comparable antimicrobial activities to the commercially obtained antibiotic, Chloramphenicol.

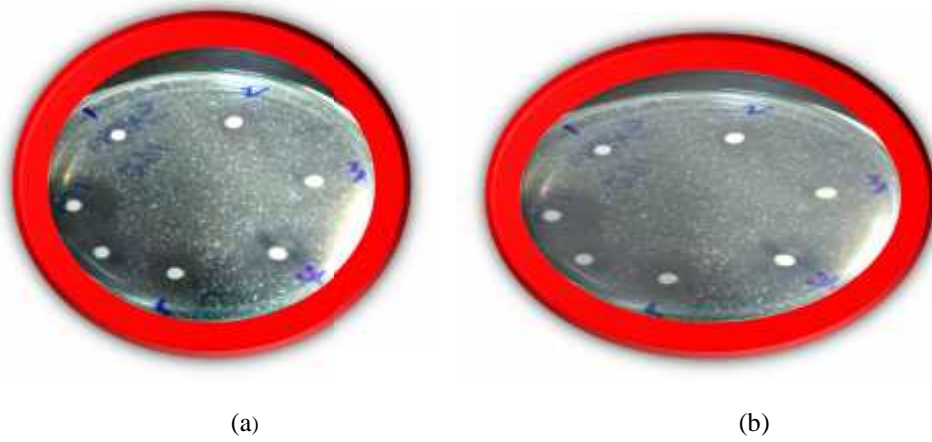


Figure 4 (a) and 4 (b). Inhibition zone of as synthesized NPs s against *Streptococcus* at the concentration of 100 (a) and 150 (b) in $\mu\text{g/mL}$ respectively.

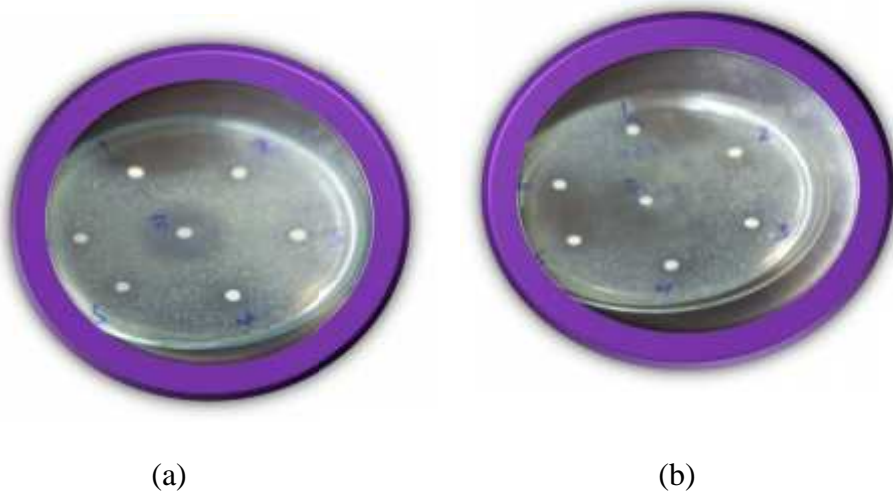
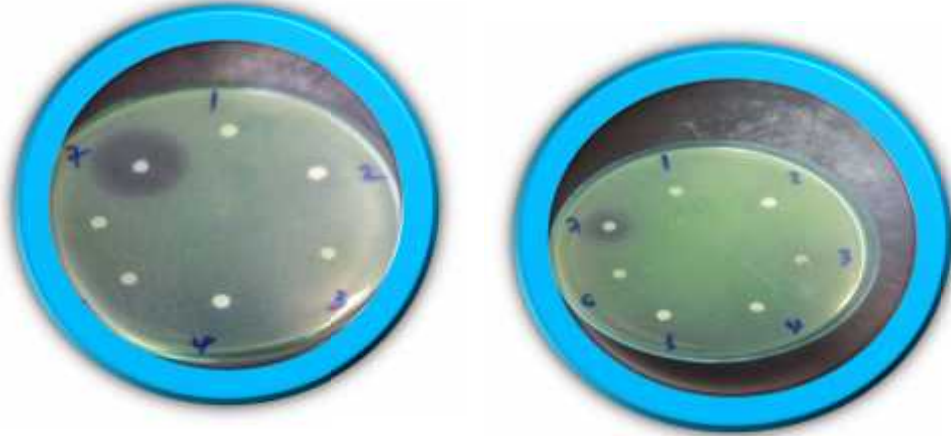


Figure 5 (a) and 5 (b). Inhibition zone of as synthesized NPs against *Escherichia coli* at the concentration of 100 (a) and 150 (b) in $\mu\text{g/mL}$ respectively.



(a)

(b)

Figure 6 (a) and 6 (b). Inhibition zone of as synthesized NPs against *Pseudomonas aeruginosa* at the concentration of 100 (a) and 150 (b) in $\mu\text{g/mL}$ respectively.

	Gram positive						Gram negative					
	<i>Staphylococcus aureus</i>			<i>Streptococcus</i>			<i>Escherichia coli</i>			<i>Pseudomonas aeruginosa</i>		
Antibiotics	50 μg/ml	100 μg/ml	150 μg/ml	50 μg/ml	100 μg/ml	150 μg/ml	50 μg/ml	100 μg/ml	150 μg/ml	50 μg/ml	100 μ/ml	150 μg/ml
ZnS	10 mm	17 mm	23 mm	0 mm	8 mm	11mm	7 mm	12 mm	17 mm	0 mm	6 mm	7 mm
CdS	9 mm	16 mm	15 mm	0 mm	6 mm	9 mm	0 mm	6 mm	8 mm	0 mm	5 mm	9 mm
NiS	0 mm	7 mm	8 mm	0 mm	6 mm	7 mm	0 mm	5 mm	6 mm	0 mm	0 mm	6 mm
ZnS/CdS	23 mm	25 mm	24 mm	13 mm	16 mm	18 mm	0 mm	7 mm	7 mm	0 mm	6 mm	9 mm
ZnS/NiS	20 mm	21 mm	27 mm	10 mm	13 mm	16 mm	0 mm	7 mm	8 mm	0 mm	6 mm	7 mm
ZnS/CdS/NiS	24 mm	27 mm	37 mm	10 mm	18 mm	22 mm	6 mm	7 nm	14 mm	0 mm	10 mm	13 mm
Chloram- phenicol	24 mm	30 mm	33 mm	26 mm	27 mm	30 mm	27 mm	29 mm	30 mm	20 mm	24 mm	28 mm

Table 2. Zone of inhibition (in mm) of different as-synthesized nanomaterials with the concentration of 50 μg/mL, 100 μg/mL and 150 μg/mL against both Gram positive (*Staphylococcus aureus* and *Streptococcus*) and Gram negative (*Escherichia coli* and *Pseudomonas aeruginosa*) bacteria.

5. SUMMARY, CONCLUSION AND RECOMMENDATIONS

5.1. Summary and Conclusion

In this work, nanoparticles of the metal sulfides (ZnS, CdS and NiS) were prepared successfully by precipitation method from the aqueous solutions of $\text{Na}_2\text{S} \cdot 9\text{H}_2\text{O}$ and their soluble salts $\text{Zn}(\text{NO}_3)_2 \cdot 6\text{H}_2\text{O}$, $\text{Cd}(\text{NO}_3)_2 \cdot 4\text{H}_2\text{O}$ and $\text{Ni}(\text{NO}_3)_2 \cdot 4\text{H}_2\text{O}$, respectively. Likewise the binary nanocomposites ZnS/CdS and ZnS/NiS were prepared by the same method, by mixing aqueous solutions of their precursors used for the preparation of ZnS and CdS as well as ZnS and NiS, respectively. Similarly, the ternary nanocomposite ZnS/CdS/NiS was prepared by precipitation method by mixing aqueous solutions of their precursors used for the preparation of ZnS, CdS and NiS.

The as-synthesized nanomaterials were characterized by Uv-Vis spectrophotometer and X-ray diffractometer (XRD) for determination of the band gap energies and crystallite sizes of the nanomaterials respectively.

The antimicrobial activities of all the synthesized nanomaterials were studied against the Gram positive (*Staphylococcus aureus* and *Streptococcus*) and Gram negative (*Escherichia coli* and *Pseudomonas aeruginosa*) bacteria using the paper disc diffusion technique. The minimum effective dose of each of the synthesized nanomaterials was found to be 150 $\mu\text{g}/\text{ml}$. This value indicates that as concentration of the material increase its antimicrobial activity against the tested bacteria increases. It was observed that the as-synthesized nanomaterials act as stronger antibiotics against Gram positive (*Staphylococcus aureus* and *Streptococcus*) bacteria than the Gram negative (*Pseudomonas aeruginosa* and *Escherichia coli*) bacteria.

The incorporation of CdS and NiS into ZnS to form ZnS/CdS/NiS nanocomposite showed a cumulative effect at improving the antimicrobial activities of ZnS, accordingly, ZnS/CdS/NiS nanocomposite exhibited a much better cumulative effect than the other as-synthesized nanoparticles and this value was almost comparable to the commercially available antibiotic (Chloramphenicol). The binary nanocomposites ZnS/CdS and ZnS/NiS also showed better antimicrobial activities than their corresponding single components.

5.2. Recommendation

- Based on the outcomes of this study, it has been recommended that further research should be carried out on the antimicrobial activities of these nanomaterials on different bacteria strains other than those mentioned in this study.
- It may be useful to synthesize the ternary nanocomposite mentioned in this study using different percentage compositions of the components.
- Further characterization required using SEM, TEM in order to know their morphology and other property as well.
- Further research on other sulfides of ternary nanocomposite will be helpful.

6. REFERENCE

- Atay, F.Ph.D. 2002. CdS: Ni Films obtained by Ultrasonic spray pyrolysis. *Thesis, Osmangazi Universtity Materials letters, 3461-3472*
- Alivisatos, P. 1996. Semiconductor clusters, nanocrystals, and Quantum dots. *Science*, 271: 933-937.
- Alin, R.R., Rozue., Shally.V. Priya Dharshini, M. and Gerardin Jayam. 2015. Structural and Optical properties of Nickel Sulphide (NiS) nanoparticles. *International Journal of NanoScience and Nanotechnology*, 6: 41-45
- Behera, P.S.J., Pramanik, K., Panda, N and Thatoi, H. 2012. Fuctionalized Magnic Nanoparticles and their effect on *Escherichia Coli* and *Staphylococcus ureus*. *World Journal of Nano Science*, 2015:10-21
- Blasco, F., Perello, L., Latorre, J., Borrás, J. and Garcia, S.G. 1996. Cobalt (II), nickel (II), and copper(II) complexes of sulfanilamide derivatives: synthesis spectroscopic studies, and antibacterial activitiy. Crystalstructure of [Co (sulfacetamide)₂(NCS)₂]. *Journal of Inorganic Biochemistiry*, 61(2): 143 - 154.
- Bither, T.A., Bouchard, R.J., Cloud, W. H., Donohue, P.C. and Siemons, W. 1968. Crystal structure, physical properties of NiS₂. *Journal of Inorganic Chemistiry*, 7: 2208-2210
- Carotenuto, G., Nicolais, L., Perlo, P. and Martorana, D. 2014. Method of production of polymer/metal or metal sulphide composites which uses metal mercaptides. *Materials Research Bulletin*, 46: 569–575.
- Chohan, Z.H. 2000. Symmetric 1,1'-dimethylferrocenederived amino acids: their synthesis, characterization, ligational and biological properties with Cu(II), Co(II) and Ni(II) ions. *Metal Based Drugs*, 7: 177 – 183.
- Coe, S., Woo, W.K., Bawendi, M. and Bulovic, V. 2002. Electro luminescence from single monolayers of nano crytals in molecular organic devices. *Nature photonics*, 420: 800-803.
- Cozzoli, P.D., Kornowski, A. and Weller, H. 2005. Nanocomposites size-tunable ZnO nanoparticles and amphiphilic hyperbranched polymers. *Journal of Physics and Chemistiry*, 109: 2638-2643.
- Du, J., Fu, L., Liu, Z., Han, B., Li, Z., Liu, Y., Sun, Z. and Zhu, D. 2005. Facile route to synthesize multi-walled carbon nanotube/zinc sulfide heterostructures: Optical and electrical properties. *Journal of Physics and Chemical Biology*, 109: 12772–12776.

- Eustis, S. and El-Sayed, M.A. 2006. Why gold nanoparticles are more precious than pretty gold: Noble metal surface plasmon resonance and its enhancement of the radiative and nonradiative properties of nanocrystals of different shapes. *Chemical Society Reviews*, 35: 209-217.
- Elidrissi, B., Addou, M., Regragui, M., Bougrine, A. and Kachoune, A. 2001. Structure, composition and optical properties of ZnS thin films prepared by spray pyrolysis. *Journal of Material Chemistry and Physics*, 68: 175–179.
- Gao, X.D. 2004. Morphology and optical properties of amorphous ZnS films deposited by ultrasonic-assisted successive ionic layer adsorption and reaction method. *Journal of thin Solid Films*, 468: 43–47.
- Gebru, H., Abi, T., Kaushik, J. and Yadav, O. P. 2003. Distinct anti-microbial effects of synthesized ZnS, Ag-N co-doped ZnS and ZnS-Fe₂O₃ composite nanoparticles against some pathogenic bacterial strains. *Journal of Surface Science and Technology*, 29: 1-20.
- Ghezelbash, A., Sigman, M. B. and Korgel, B. A. 2004. Solventless synthesis of nickel sulfide nanorods and triangular nanoprisms. *Nano Letters*, 4: 537–542.
- Ghrayeb, J., Jackson, T.W., Daniels, R. and Hopper, D.G. 1997. Impedance study of Nano structure cadmium sulfide and zinc sulfide. *Archives of applied science research*, 2(3): 225-230.
- Gupta, M. and Sharma, V. 2011. Targeted drug delivery system. *A Review Research Journal of Chemical Science*, 1(2): 135-138.
- Gutierrez, F.M., Olive, P.L., Banuelos, A., Orrantia, E., Nino, N., Sanchez, E.M., Ruiz, F., Bach, H. and Gay, Y.A. 2010. Synthesis, characterization, and evaluation of antimicrobial and cytotoxic effect of silver and titanium nanoparticles. *Journal of Nanomedicine*, 6: 681-688
- Hitanshu, K.P.B., Barman, G. and Ragini, R.S. 2014. Development of CdS, ZnS Quantum Dots and their Core/Shell Structures by wet chemical method. *Applied Physics*, 117: 1249-1258.
- Huang, L., Wang, X., Yang, J., Liu, G., Han, J. and Li, C. 2013. Dualcocatalysts loaded type I CdS/ZnS core/shell nanocrystals as effective and stable photocatalysts for H₂ evolution. *Journal of Physics and Chemistry*, 117: 11584–91
- Jamieson, T., Bakhshi, R., Petrova, D., Pocock, R., Imani, M. and Seifalian, A.M. 2007. Biological applications of quantum dots. *Journal of Biomaterials*, 28: 4717-4732.
- Kaltenhauser, V., Rath, T., Haas, W., Torvisco, A., Muller, S.K., Friedel, B., Kunert, B., Saf, R., Hofer, F. and Trimmel, G. 2013. Bismuth sulphide-polymer nanocomposites from a highly soluble bismuth xanthate precursor. *Journal of Material Chemistry*, 1: 7825–7832.

- Kamalakannan, P. and Venkappayya, D. 2002. Synthesis and characterization of cobalt and nickel chelates of 5-dimethylaminomethyl-2-thiouracil and their evaluation as antimicrobial and anticancer agents. *Journal of Inorganic Biochemistry*, 90: 22-37.
- Kansal, S.K. 2007. Photocatalytic decolourization of direct yellow 9 on titanium and zinc oxides. *Journal of Hazardous Materials*, 141(31): 581-590.
- Klimov, V.I., Mikhailovsky, A.A., Xu, S., Malko, A.H., J.A., Leatherdale, C.A., Eisler, H.J. and Bawendi, M.G. 2006. Optical gain stimulated emission in nanocrystal quantum dots. *Science*, 290: 314-323
- Mamta Yadav., Ali, S. and Yadav, O.P. 2014. Distinct anti-microbial effects of synthesized ZnS, Ag-N co-doped ZnS and ZnS-Fe₂O₃ composite nanoparticles against some pathogenic bacterial strains. *Journal of surface science and technology*, 5(6): 34-41.
- Martinez. S., Gomez, I., Hinojosa, M., Kharissova, O.V. and Hernandez, T. 2010. Highly Luminescent ZnS Nanoparticles Obtained by Microwave Heating. *Synthetic Reaction in Inorganic Materials Chemistry*, 40: 455-464.
- Nanda, J.K., and Sarma, D.D. 1999. Photoelectron spectroscopic study of CdS nanocrystallites. *Physical Review Letters*, 59: 7473-7479.
- Nayereh Soltani., Elham Gharibshahi and Elias Saion. 2012. Band gap of Cubic and Hexagonal CdS Quantum Dots Experimental and Theoretical Studies. *Chalcogenide Letters*, 9(7): 321 - 328.
- Olumide Oluwale Akinwunmi¹., Gabriel O. Egharevba and Ezekiel Oladele Bolarinwa Ajayi¹. 2014. Synthesis and Characterization of CdS, ZnS and CdZnS Nanoparticles Embedded in Polystyrene. *Journal of Modern Physics*, 5: 257-266.
- Parak, W.J., Gerion, D., Pellegrino, T., Zanchet, D., Micheel, C., Williams, C.S., Boudreau, R., Le, Gros, M.A., Larabell, C.A. and Alivisatos, A.P. 2003. Biological applications of colloidal nanocrystals. *Nanotechnology*, 14:15-27.
- Pooja, S. and Lunawat, N. 2007. International Journal of Hydrogen Energy, *International conference on materials for hydrogen energy*, 14(32): 2607-3108.
- Popova, T.P., Alexandrova, R.I., Tudose, R., Mosoarca, E.M. and Costisor, O. 2014. Antimicrobial activity in vitro of four nickel complexes. *Journal of biotechnology*, 5 (5): 255-261
- Rao, N. S. and Reddy, M.G. 1990. Studies on the synthesis, characterization and anti-microbial activity of new Co (II), Ni(II) and Zn(II) complexes of Schiff base derived from ninhydrin and glycine. *Biology of Metals*, 3(1): 19 - 23.

- Ranjbar, M., Yousefi, M., Nozari, R. and Sheshmani, S. 2013. Synthesis and characterization of cadmium-thioacetamide nanocomposites using a facile sonochemical approach: A precursor for producing Cds nanoparticles via thermal decomposition. *International Journal of Nanoscience and Nanotechnology*, 9: 203–212.
- Sarita, N. 2010. Synthesis, Characterization and applications of CdO, CdS nanoparticles and nanocomposites. *Thesis, shoolini University of biotechnology*, 57-58.
- Saxena, A., Tripathi, R. M. and Singh, R. P. 2010. Biological synthesis of silver nanoparticles by using onion (*Allium cepa*) extract and their Antibacterial activity. *Digest journal of nanomaterials and biostructures (DJNB)*, 52: 145-156.
- Sarmila Dutta., Shibabrata., Basak and Pijus Kanti Samanta. 2012. Enhanced photo luminescence from ZnO/ZnS core-shell structure. *Journal of Chemical Engineering and Materials Science*, 3(2): 18-22.
- Senapati, U.S., Jha, D.K. and Sarkar, D. 2013. Distinct anti-microbial effects of synthesized ZnS, Ag-N co-doped ZnS and ZnS-Fe₂O₃ composite nanoparticles against some pathogenic bacterial strains. *Journal of Physical Science*, 1(7): 1-6.
- Senthilkumar, S. and Selvi, T.R. 2008. Synthesis and characterization of one dimensional ZnS nanorods. *Synthetic Reaction in Inorganic Meterials Chemistry*, 38: 710–715.
- Shivankar, V.S. and Takkar, N.V. 2003. Synthesis, characterization and antimicrobial activity of some mixed ligand Co(II) and Ni(II) complexes. *Acta Poloniae Pharmacectical*, 60(1): 45-50
- Singh, C.P., Bindra, K.S. and Oak, S.M. 2010. Nonlinear optical studies in semiconductor-doped glasses under femto second pulse excitation. *Pramana Journal of Physics*, 75: 1169–1173.
- Shubhangi, D., Bompilwar¹, Subhash., Kondawar, B., Vilas., and Tabhane, A. 2010. Impedance Study of Nanostructure Cadmium Sulfide and Zinc Sulfide. *Archives of Applied Science Research*, 2 (3): 225-230
- Sun, S., Murry, C.B., Weller, D., Folks, L. and Moster, A. 2000. Mono disperse FePt nano -particles and Ferromagnetic FePt nanocrytal superlattices. *Science*, 287: 1989-1992
- Tittel, J.W., Gohde, F., Koberling, Th., Basche, A., Kornowski, H., Weller, A. and Eychmuller. 2009. Transition temperature of PMMA and CdS-PMMA composite. *Chalco Letter*, 6:55-67.
- Weller, H. 1993. Quantized semiconductor particles and a novel state of matter for materials science. *Advanced Material*, 5: 88–95.

Zhang, C.Q., Sun, J., Wang, W., Yang, Q.B., Li, Y.X. and Du, J.S. 2012. Facile method to prepare metalsulfide (Ag_2S , CuS , PbS) nanoparticles grown on surface of polyacrylonitrile nanofibre and their optical properties. *Chemistry Research Chiana University*, 28: 534–538.

7. APPENDIX

Appendix Table 1. Wave length (nm) and absorbance (a.u) for Uv-Vis absorption spectrum of ZnS, CdS, NiS, ZnS/CdS, ZnS/NiS and ZnS/CdS/NiS .

Wave length in nm	Absorbance of Nanoparticles.					
	ZnS	CdS	NiS	ZnS/CdS	ZnS/NiS	ZnS/CdS/NiS
650	0.01	0.021	0.219	0.03	0.01	0.04
645	0.023	0.027	0.219	0.943	0.182	0.851
640	0.023	0.027	0.219	0.941	0.183	0.852
635	0.023	0.027	0.220	0.939	0.184	0.853
630	0.023	0.028	0.220	0.936	0.185	0.855
625	0.024	0.028	0.220	0.934	0.187	0.857
620	0.024	0.028	0.220	0.932	0.188	0.859
615	0.024	0.028	0.220	0.930	0.19	0.86
610	0.024	0.028	0.220	0.928	0.192	0.861
605	0.025	0.029	0.221	0.926	0.194	0.862
600	0.025	0.029	0.221	0.926	0.196	0.863
595	0.025	0.029	0.222	0.925	0.198	0.864
590	0.025	0.030	0.222	0.926	0.20	0.865
585	0.025	0.031	0.223	0.926	0.203	0.866
580	0.025	0.032	0.223	0.926	0.206	0.868
575	0.025	0.033	0.224	0.926	0.209	0.870
570	0.025	0.034	0.224	0.926	0.211	0.871
565	0.026	0.034	0.225	0.927	0.214	0.873
560	0.026	0.035	0.225	0.927	0.217	0.875
555	0.026	0.036	0.225	0.926	0.22	0.876
550	0.026	0.036	0.225	0.925	0.223	0.878
545	0.026	0.037	0.225	0.925	0.226	0.88
540	0.026	0.038	0.226	0.925	0.229	0.882
535	0.026	0.039	0.226	0.924	0.232	0.884
530	0.026	0.04	0.226	0.924	0.235	0.887
525	0.027	0.041	0.227	0.924	0.238	0.89
520	0.027	0.043	0.227	0.925	0.241	0.893
515	0.027	0.045	0.227	0.926	0.244	0.897
510	0.027	0.047	0.227	0.927	0.247	0.901
505	0.027	0.049	0.228	0.928	0.250	0.905
500	0.027	0.052	0.228	0.930	0.253	0.91
495	0.028	0.055	0.228	0.932	0.257	0.916
490	0.028	0.066	0.228	0.935	0.260	0.922
485	0.028	0.076	0.228	0.939	0.263	0.929
480	0.028	0.089	0.227	0.943	0.267	0.936
475	0.028	0.107	0.227	0.946	0.271	0.944

470	0.029	0.129	0.227	0.948	0.275	0.951
465	0.029	0.156	0.227	0.951	0.280	0.958
460	0.029	0.185	0.226	0.954	0.284	0.964
455	0.03	0.213	0.226	0.958	0.290	0.969
450	0.031	0.236	0.226	0.961	0.296	0.974
445	0.032	0.252	0.226	0.965	0.302	0.978
440	0.033	0.256	0.226	0.970	0.309	0.981
435	0.034	0.241	0.226	0.975	0.316	0.985
430	0.034	0.2	0.225	0.981	0.324	0.987
425	0.035	0.156	0.225	0.988	0.331	0.99
420	0.036	0.12	0.225	0.995	0.339	0.993
415	0.036	0.125	0.225	1.004	0.348	0.996
410	0.037	0.141	0.225	1.014	0.357	1.00
405	0.038	0.154	0.225	1.024	0.366	1.003
400	0.039	0.159	0.225	1.035	0.374	1.006
395	0.04	0.225	0.225	1.045	0.382	1.009
390	0.041	0.225	0.225	1.056	0.388	1.012
385	0.043	0.226	0.226	1.065	0.395	1.013
380	0.045	0.226	0.226	1.073	0.400	1.014
375	0.047	0.226	0.226	1.079	0.406	1.014
370	0.049	0.227	0.227	1.083	0.413	1.014
365	0.052	0.229	0.229	1.086	0.424	1.014
360	0.055	0.225	0.234	1.091	0.442	1.016
355	0.06	0.225	0.246	1.097	0.474	1.02
350	0.066	0.225	0.272	1.106	0.532	1.029
345	0.076	0.225	0.329	1.123	0.635	1.052
340	0.089	0.225	0.436	1.157	0.81	1.098
335	0.107	0.225	0.618	1.224	1.083	1.185
330	0.129	0.226	0.780	1.334	1.469	1.322
325	0.156	0.226	0.90	1.496	1.962	1.521
320	0.185	0.226	0.89	1.700	2.354	1.765
315	0.213	0.225	0.78	1.901	2.375	1.995